

F. N. Coton & R. A. McD. Galbraith
University of Glasgow

1.0 Introduction

Abstract

The paper describes a direct scheme for the prediction of laminar separation bubbles. It was hoped that it would provide a criterion for transition on low Reynolds number aerofoils. The method was found to be sensitive to the empirical input of pressure distribution with implied fixed transition and, indeed, minor physically realistic modifications to it yielded significant effects on the predicted lift values. It is postulated that inverse methods tackling a similar problem will have comparable sensitivity which renders both schemes to have an accuracy dependent on the empirical inputs chosen. The current method has value in the ease with which future investigations and postulations of bubble development may be made.

Nomenclature

CD	Dissipation coefficient
C _f	Skin friction coefficient
C _L	Lift coefficient
C _{mq}	Pitching moment coefficient about quarter chord
C _p	Pressure coefficient
D	Dissipation integral
H	Momentum form parameter δ^*/θ
H _e	Energy form parameter ϵ/θ
L	Ordinate of Le Foll's plane
l _T	Separated laminar shear layer length
Rc	Chord Reynolds number
R _θ	Momentum thickness Reynolds number
s, y	Coordinates along and normal to surface
TF	Taylor's Turbulence Factor
u, v	Velocities within the boundary layer in the s, y directions
u', v'	Boundary layer fluctuation velocities in the s, y directions
U ₀	Freestream velocity
u _e	Velocity at edge of boundary layer
X	Abscissa of Le Foll's plane
δ	Boundary layer thickness
δ*	Boundary layer displacement thickness
ε	Boundary layer energy thickness
θ	Boundary layer momentum thickness
ν	Kinematic viscosity

Subscripts

sep	Separation
s	Surface distance

Copyright © 1988 by ICAS and AIAA. All rights reserved.

The prediction of aerofoil performance at low Reynolds numbers is complicated by the need for accurate transition models. Of particular relevance is the performance in the region of the stall where the turbulent boundary layer is very sensitive to the manner of transition. This sensitivity is because the development of the turbulent boundary layer is inextricably linked to its 'starting' conditions which will differ depending on the transition model employed.

Physically, the transition mechanisms most often considered include the laminar separation bubble, fixed transition by means of a wire trip or roughness elements and 'natural' transitions. Each of these mechanisms will generate a different turbulence structure at the start of the turbulent boundary layer and so the layers subsequent development will be influenced by transition type. This is a result of the so called 'history effects' in which the layer does not react instantaneously to local conditions^(1,2), but has within it a carry over from upstream conditions. Also, as discussed by Head⁽³⁾, even in conditions conducive to the development of equilibrium boundary layers, the layers development is influenced by starting conditions. For some equilibrium cases, a divergence towards separation was evident instead of a convergence to the equilibrium state.

This phenomena often accounts for discrepancies between various wind tunnel investigations of the same aerofoil⁽⁴⁾. For moderate incidences, where there is little trailing edge separation, the disparities are small. As the separation penetrates towards the leading edge, however, the sensitivity of the transition mechanism is most marked. This may also be the case for prediction codes and, indeed, Coton & Galbraith⁽⁵⁾ were led to this conclusion from the results depicted in Fig 1.

This figure illustrates the agreement between the measured and predicted characteristics of a NACA 4415 aerofoil for various Reynolds numbers. It may be observed, that for the lowest Reynolds number considered, there is a systematic difference between the measured and predicted values in the region of stall. One can speculate that this result may have been influenced by an inappropriate starting condition for the turbulent boundary layer.

The particular performance code used in Fig 1 indicated the existence of short leading edge bubbles at the higher incidences. For this case, however, transition was fixed at the location of laminar separation with a turbulent boundary layer starting profile appropriate to the local form parameter taken from the Coles⁽⁶⁾ family. At the

2. Viscid-Inviscid Scheme with Incorporated Separation Bubble Calculation

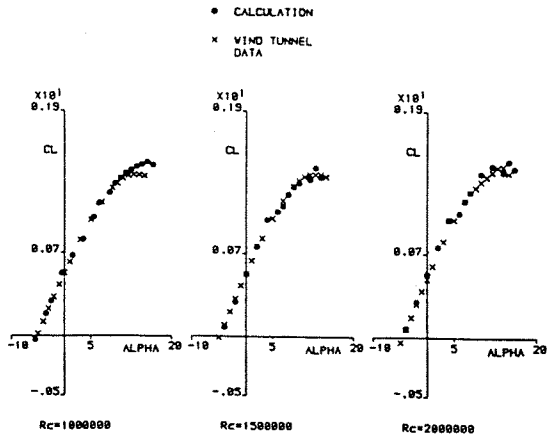


FIGURE 1. Comparison of calculated lift coefficients with wind tunnel data for the NACA 4415 aerofoil at three Reynolds numbers.

larger Reynolds numbers, where the bubble may have been very short, this transition criterion appears to have had little effect. As the Reynolds number is reduced, however, the bubble extends and the calculation may be less valid. The resulting predicted overestimate of C_L , therefore, may be a consequence of an inappropriate turbulent boundary layer starting location and profile; the current criterion has a fuller velocity profile than that for re-attachment. If it were possible to calculate through the bubble and predict more appropriate starting conditions, then the above problem may be alleviated resulting in increased confidence in performance predictions for design purposes.

The paper describes a direct bubble prediction code developed for the purposes of investigating the above speculations with regard to Fig 1. It is shown that, when compared to the momentum thickness development obtained by forcing transition at the location of laminar separation, the value acquired from the bubble calculation may be either greater or less, depending on the particular flow conditions and bubble assumptions invoked. In an extreme case the value of momentum deficit thickness can be as much as three times that from the simple algorithm. It can be accepted therefore, that with the bubble algorithm employed, one could expect significant differences in predicted aerofoil performance.

The resultant predictions, however, are inconclusive, save only that they highlight the great importance of transition modelling within the free shear layer. With minor and physically realistic modifications to the transition model, significant changes to the predictions occur. Comparing the present direct technique with several extant inverse bubble calculations^(7, 8, 9), it is postulated that they too will be sensitive to the transition criterion in a similar way. It is felt, however, that the new direct bubble predictions algorithm offers a tool by which bubble models and techniques may be investigated with a clarity hitherto unavailable.

The routines relevant to the modelling of the separation bubble phenomenon were originally envisaged as being supplementary to the viscid-inviscid interaction scheme of Coton and Galbraith⁽⁵⁾. In this way, it was possible to obtain a fully converged solution of the main interaction scheme for, say, a calculation with transition fixed at the point of laminar separation, before initiating a study of the effects of any indicated separation bubble. For higher Reynolds numbers, where the effect of such a bubble may be expected to be less significant⁽⁴⁾, the calculation could, therefore, be terminated after the initial solution was obtained. This approach offered computational efficiency since, during the initial interaction stages, the boundary layer calculation was considerably faster without the separation bubble model invoked.

2.1 Description of the Basic Viscid-Inviscid Interaction Scheme

When separated aerofoil flows are modelled by means of a viscid-inviscid interaction method, the boundary layer equations are required to be 'matched' to an inviscid calculation⁽¹⁰⁾. In the direct mode, this is achieved by iteratively accounting for the displacement effect of the boundary layer, either by adjusting the aerofoil shape or by introducing an equivalent source distribution into the inviscid calculation; the sequence of this is as indicated in Fig. 2. It is the former technique that is employed herein.

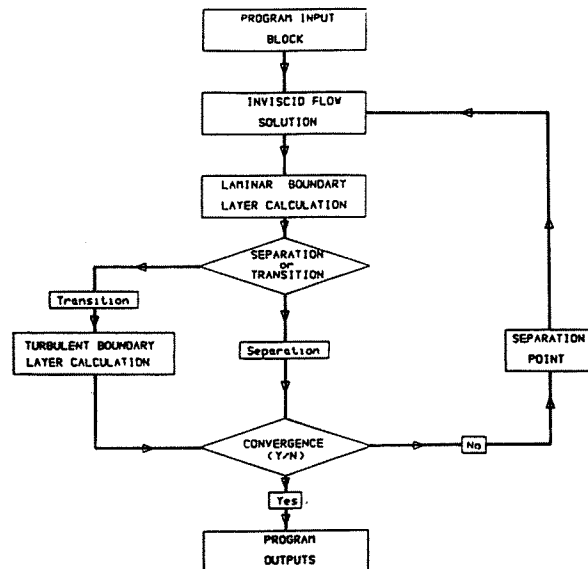


FIGURE 2. Viscid-inviscid interaction scheme flow chart

In this method, boundary layer displacement effects are only included when the calculation appears to be nearing convergence. This approach results in a rapid initial convergence followed by final small corrections, producing consistent results. The method is capable of assessing the performance of aerofoils with either turbulent boundary layer separation towards the trailing edge or, at low Reynolds number, separations associated with the laminar boundary layer close to the leading edge.

Use is made of the algorithm developed by Leishman et al⁽¹¹⁾, which exhibits the essential features of the method of Dvorak & Maskew⁽¹²⁾, to model the inviscid flowfield. In it, the aerofoil profile is replaced by an inscribed polygon of vortex panels over which the vorticity varies linearly, achieving piecewise continuity between adjoining panels. The free shear layers used to model the aerofoil wake comprise of uniform strength vorticity panels. The distribution of these panels is indicated in Fig. 3.

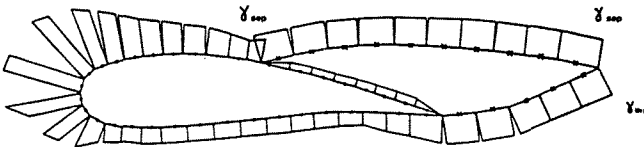


FIGURE 3. Aerofoil vortex panel distribution for separated flow

The modelled wake region is assumed to be inviscid with negligible vorticity and is taken to have a constant total pressure equal to that at separation. It is further assumed that the free shear layers have no significant thickness and can be represented as streamlines across which there exists a velocity jump.

Each panel contains a control point at which the condition of flow tangency is applied. This is achieved by setting the scalar product of the induced velocity with the surface normal vector, to zero. This yields a set of linear simultaneous equations which, in conjunction with a specified Kutta condition, may be solved to yield the strength of the assumed vortex sheets, from which the required velocity distribution is obtained.

As part of the inviscid procedure, the wake shape is iteratively obtained from an initial shape estimate. The degree of correspondance which exists between the modelled and actual wake shape influences the acceptability of the final prediction⁽¹¹⁾. Dvorak and Maskew⁽¹²⁾ established that a practical initial wake shape may be obtained, by representing the location of the upper and lower free shear layers by parabolic curves with a common intersection point in the freestream. The shape of these curves is constrained by a Wake Factor; defined as the ratio of the wake length to wake height. During the iterative process, the free vortex sheets of the wake are continually adjusted until they fall on a streamline. Three wake iterations are normally

required, although up to six may be necessary for large areas of separated flow, due to the deterioration of the validity of the initial wake shape estimate.

The laminar and turbulent boundary layer calculations are integral techniques based on the method of Le Foll⁽¹³⁾. This procedure requires the simultaneous solution of the momentum and energy integral equations over each calculative step. These equations are cast in the form of Assassa and Papailiou⁽¹⁴⁾ and are solved in the direct mode.

The laminar method utilises relations derived from the velocity profile family of Head to provide skin friction and dissipation coefficient values and to effect closure of the system of equations.

For the turbulent boundary layer, Coles⁽⁶⁾ velocity profile family, in the more generalised form of Khun and Neilsen⁽¹⁵⁾, is used, together with the Nash π -G relationship⁽²⁾, to provide the velocity profiles and skin friction at each station in the calculation and to effect closure.

2.2 Separated Flow Boundary Layer Calculation

Extension of the boundary layer calculation through the point of laminar separation was hampered by the existence of the well documented⁽¹⁴⁾ singularity which results in a breakdown of the direct boundary layer calculation as separation is approached. Recent investigations^(7,9) have preferred to calculate through the point of laminar separation by solving the boundary layer equations in the inverse mode. When a solution is obtained in this manner, the velocity distribution is the calculation output with some parameter such as displacement thickness taken as an initial specified input. This approach exhibits no singular behaviour around the separation point and, as such, a smooth progression from attached to separated flow is obtained. For the calculation of separation bubble effects, the inverse formulation requires a fully viscid-inviscid interaction type approach with, generally, the final result particularly sensitive to the boundary layer and transition models.

The recent direct turbulent boundary layer calculation technique of Assassa and Papailiou⁽¹⁴⁾ has been shown to behave well in the vicinity of separation and has been used successfully to calculate small regions of separated flow. The good performance of this method around the separation region is principally due to the manner in which the momentum and energy integral equations are formulated, with the chosen boundary layer variables being finite and well behaved near separation. The ability of this method to predict a reattaching boundary layer⁽¹⁴⁾, indicated it's suitability for application to the turbulent portion of a separation bubble. Calculation of the laminar portion of the shear layer still posed a significant problem if the direct approach were to be employed.

The previously discussed direct laminar

boundary layer calculation technique was well behaved as separation was approached. It was therefore felt that an investigation into the possible extension of the method through the point of laminar separation was warranted by the success of the above turbulent method. In the calculation scheme, the momentum and energy equations are solved simultaneously over each stepwise increment. These equations (1 & 2), which are solved in the direct mode, are cast in the form of Assassa and Papailiou⁽¹⁴⁾.

$$dq = C_1 dL - \frac{C_1 M}{1 + 2C_1 M} dX \quad (1)$$

$$d\phi = \frac{e^X dX}{(1 + 2C_1 M) CD e^{2C_1 L}} \quad (2)$$

During the calculation, the values of $d\phi$ and dq , corresponding to the increment in stepsize Reynolds number and the velocity gradient respectively, are necessary inputs. The boundary layer development is given by the change in Reynolds number based on a boundary layer characteristic length (dX) and the increment in the value of a profile form parameter (L). The following definitions apply :-

$$C_1 M = \frac{1}{H - 1} \left[1 - \frac{H_e C_f}{2 CD} \right] \quad (3)$$

$$X = \ln \left[\frac{\epsilon u_e}{v} e^{2C_1 L} \right] \quad (4)$$

$$dL = \frac{1}{H - 1} \frac{dH_e}{H_e} \quad (5)$$

$$\phi = \int_0^s \frac{u_e}{v} ds \quad (6)$$

$$q = \ln \frac{u_e}{U_0} \quad (7)$$

The functions L and X are well behaved at separation which, for both the laminar and turbulent calculations, is indicated by vanishing skin friction.

2.2.1 Laminar Boundary Layer

In the attached flow laminar boundary layer calculation, form parameter relations along with

skin-friction and dissipation coefficient functions derived from Head's velocity profile family are used to effect closure of the above system of equations. Unfortunately, the velocity profile family only contained profiles indicative of attached flow. It was therefore necessary to extend the range of profiles in order that the required function relationships could be developed for separated flow.

To retain consistency between the profiles developed by Head⁽¹⁶⁾ and those to be developed for the separated flow calculation, the same basic approach that Head used was employed. In it, the Blasius profile is incremented by varying amounts of two functions derived from known profiles. By adopting this approach, a family of velocity profiles may be generated.

When considering the problem of separated flow, it was necessary to have two separated flow profiles to develop the required functions and to thus extend the velocity profile family. Empirical data for separated laminar flows was not readily available and, until recently, prone to severe measurement errors. The hypothetical separated flow profiles of Stewartson⁽¹⁰⁾, derived from solutions of the Faulkner Skan equation, however, provided ideal examples for the present purpose since the profiles were well defined and their derivatives easily obtainable. Two of these profiles were used to extend the range of the velocity profile family to include separated flows.

Once the profile shapes, indicative of separated flow, had been established, it was possible to obtain all the relevant boundary layer parameters by integration of the profiles. In this way, the required boundary layer parameter relations could be created. The developed form parameter and dissipation coefficient functions are shown in Figs. 4 & 5. A similar relation was derived for skin-friction.

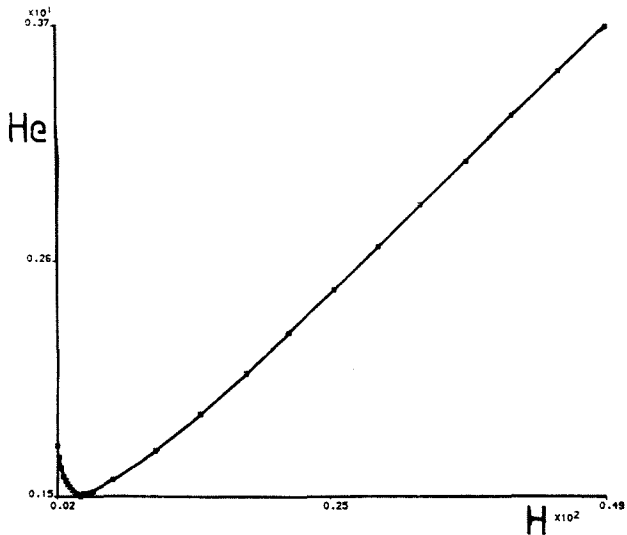


FIGURE 4. Spline-fit representation of the H-He relation.

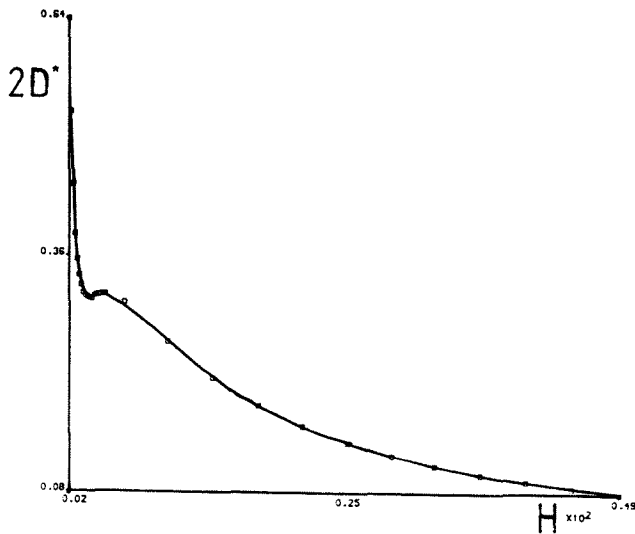


FIGURE 5. Spline-fit representation of the H-2D* relation.

2.2.2 Turbulent Boundary Layer Calculation

For the turbulent boundary layer, Coles⁽⁶⁾ velocity profile family (in the more generalised form of Khun and Neilsen⁽¹⁵⁾) was used to provide the velocity profiles and skin-friction values at each station in the calculation. The value of the dissipation coefficient is obtained via a semi-empirical relationship⁽¹⁴⁾ which was derived using the π -G relationship. The influence of the second order terms, i.e. normal stresses, on the turbulent boundary layer calculation is included by setting the value of the constant C_1 to 0.85, i.e.

$$C_1 = \frac{H - 1}{H^* - 1} = 0.85 \quad (8)$$

Where

$$H^* = \frac{\delta^*}{\theta^*} \quad (9)$$

And

$$\theta^* = \theta - \int_0^{\delta} \frac{\overline{u'^2} + \overline{v'^2}}{u_e} dy \quad (10)$$

The second order terms can be neglected by assigning the value of unity to C_1 in the laminar boundary layer calculation.

2.2.3 Transition

The model used to predict the transition location of the separated laminar shear layer is that due to Roberts⁽¹⁷⁾. This relation is similar to the method of Horton⁽¹⁸⁾, but takes into account the effects of freestream turbulence. The correlation can be expressed as

$$\frac{f_T}{\theta_{sep}} = \frac{K \log_{10} [\text{COTH} (TF \times 10)]}{R\theta_{sep}} \quad (11)$$

where TF is the Turbulence factor and K is a constant taking the value 2.5×10^4 . Turbulence intensity may be substituted for Turbulence Factor since, during an experiment, it is common to measure only the turbulence intensity and since, generally, the macroscale length of flow turbulence has a very small effect on the value of the Turbulence Factor. The above relation is employed in the present technique with the value of K adjusted to 3.0×10^4 to give improved agreement with available empirical data.

2.3 Boundary Layer Calculation Test Cases

The inverse calculation of Gleyzes et al, for the enlarged leading edge case, provided a test case for the developed full boundary layer technique. The pressure distribution calculated via the inverse scheme was used as the input to the direct boundary layer calculation scheme. This pressure distribution was represented by spline-fit through a number of discrete points. The results of the direct calculation are compared with the inverse solution in Fig 6.

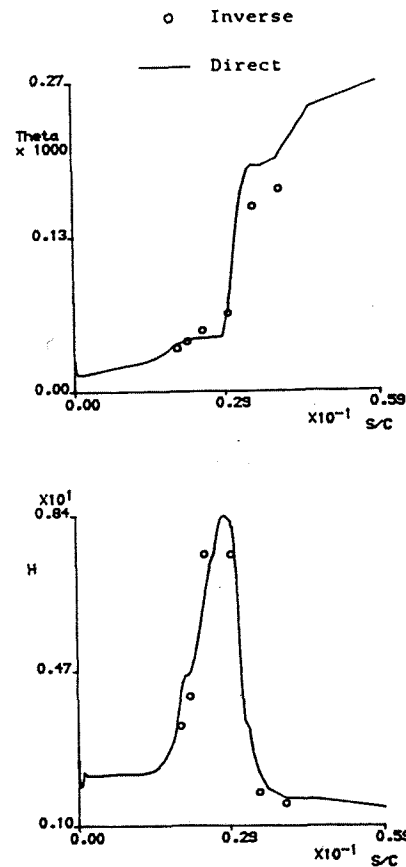


FIGURE 6. Momentum thickness and form parameter predictions compared with the inverse solution for the enlarged leading edge case of Gleyzes et al.

It is clear from the figure that the direct calculation predicted slightly higher values of momentum thickness growth, associated with the turbulent part of the separation bubble, than the calculation of Gleyzes et al⁽⁷⁾. The associated rate of decrease from the peak value of form parameter was also somewhat slower in the direct calculation. It is of significance, however, that the general form of the two predictions was very similar and that no difficulty was encountered at separation or reattachment in the direct case.

The discrepancies between the direct and inverse solutions may have arisen from two sources, the first of which was the quality of the spline fit representation of the pressure distribution. It was found that the boundary layer parameter prediction obtained, in the separation bubble, was influenced by the specification of the pressure distribution. This was particularly pertinent to the transition location where the value of form parameter was especially sensitive and would often increase after transition, contrary to experimental observation⁽⁷⁾, if the adverse pressure gradient was insufficient.

The second reason for disparity between the inverse and direct boundary layer calculations comes from the empiricism present in the two methods. It is true, as has been demonstrated for attached flow, that the empiricism and closure hypothesis employed in a specific turbulent boundary layer calculation technique, may produce results unique to that particular method. For separated flow, such effects are likely to strongly influence the obtained result which may be further affected by the non-equilibrium nature of the flow.

A comparison was also made with the predictions of Davis et al⁽⁸⁾ for the NACA 66₃-018 aerofoil originally tested by Gault⁽¹⁹⁾. As in the previous test, the velocity distribution output from the inverse calculation, which was in close agreement with the measured data, was used as the input to the direct scheme. In this case, however, it was found that the direct laminar boundary layer calculation did not predict laminar separation at the same location as the inverse scheme. This result is in agreement with the findings of Gault⁽¹⁹⁾ who also carried out a boundary layer calculation for this aerofoil and found that the predicted separation point lay well behind the measured location. As a result of the previous success of the prediction scheme used by Gault, it was concluded that the empirical data should be treated with some caution.

To obtain a comparison, it was, therefore, necessary to increase the magnitude of the adverse pressure gradient just prior to the separation point in order that the predicted direct and inverse separation points should be consistent. The adjusted pressure distribution, along with the original inverse prediction, is presented in Fig. 7. The laminar portion of the adjusted distribution was taken to have a constant pressure.

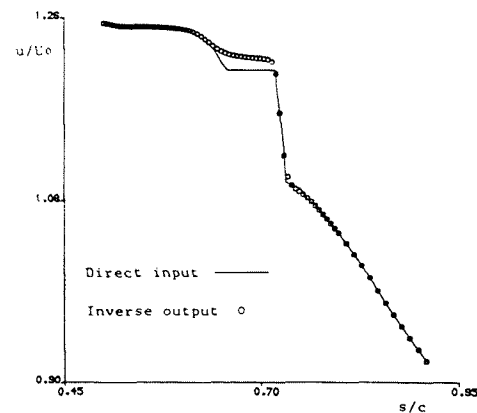


FIGURE 7. Comparison of the velocity distribution output from the inverse scheme and direct calculation input, for the NACA66₃-018 aerofoil case considered by Davis et al.

The results of the direct calculation compared with the inverse solution are presented in Fig. 8. It was considered that the results from the direct calculation, although somewhat artificial, were similar in form to the inverse solution with the greatest discrepancy occurring over the adjusted laminar portion of the bubble. The disagreement between the two attached laminar boundary layer skin friction predictions was significant. This may have been due to an over-prediction by the inverse code which, when compared to empirical data⁽⁸⁾, has been shown produce higher than expected values of skin friction.

Considerable agreement was obtained between the predicted momentum thicknesses. The variation of form parameter was also of a similar form to the inverse solution but, due to the adapted input velocity distribution, did not achieve the required growth rate in the laminar portion. The behaviour of the form parameter around transition was again found to be very sensitive to the velocity distribution specification.

In the above calculations, no difficulty was experienced when passing through the separation or reattachment points.

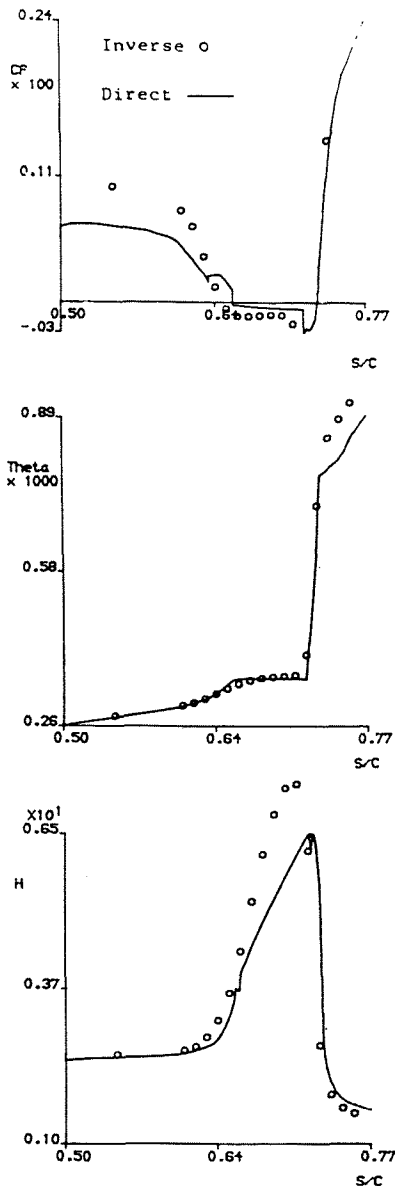


FIGURE 8. Comparison between direct and inverse boundary layer parameter predictions for the NACA66₃-018 aerofoil.

2.4 Incorporation of the Bubble Calculation into the Interaction Scheme

To perform a direct boundary layer calculation, an external velocity distribution is required as input, e.g. in the previous two cases, the input velocity distribution was provided by the output from an inverse calculation. To incorporate the separated flow boundary layer calculation into the viscid-inviscid interaction scheme, it was necessary to develop a method of prescribing the velocity distribution over the bubble.

The simple method derived by Horton⁽¹⁸⁾ to predict the growth and bursting of laminar separation bubbles has been demonstrated⁽¹⁷⁾ to provide a velocity distribution, over a separation bubble, similar to that obtained by experiment. An investigation was therefore conducted to assess the effect which such a distribution would have on the subsequent turbulent boundary layer growth as predicted by the direct calculation scheme.

Once a converged solution of the basic viscid-inviscid interaction scheme had been obtained, the size of the separation bubble could be calculated, from the value of $R_{\theta sep}$ and the velocity at separation, via Horton's method. The bubble velocity distribution could then be included into the global velocity distribution, and a calculation performed to assess the resultant boundary layer growth. With the new location of separation, the resultant inviscid pressure distribution may be calculated and the process repeated until convergence or movement of the separation point is within a prescribed limit. In reality, as may be seen from Fig. 9., iteration is seldom required.

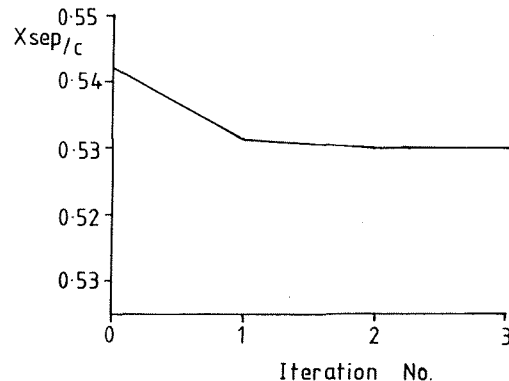


FIGURE 9. Separation point convergence history for bubble included iterations.

3.0 Results and Discussion

All the results discussed in the paper relate to the single case depicted in Fig. 1. for the NACA 4415 aerofoil at $R_c = 1000000$. It was found that these data are particularly useful for illustrating the results of the present work.

In Fig. 10. a comparison of the momentum thickness and form parameter development predicted by the method, with and without incorporated bubble calculation is given for 14.5 degrees incidence. The salient features of this result are that the momentum thickness development due to the bubble calculation, albeit significantly different in the bubble region, has a lower growth rate in the attached turbulent boundary layer than the simpler case of fixed transition at laminar separation. A similar result was observed by Gleyzes et al.⁽⁷⁾ for some cases, but, in general, the opposite would be expected⁽⁴⁾. Additionally, there is a very large form parameter peak at transition, which is comparable to inverse calculations. The sharpness of this peak, however, which is related to the corner on the

imposed pressure distribution, differs significantly from the more rounded shape associated with both inverse calculations and experiment.

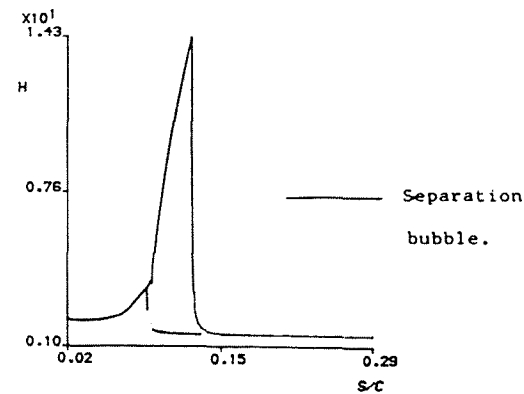
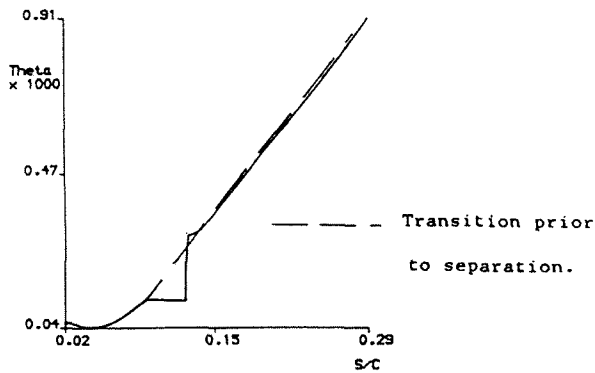


FIGURE 10. Comparison between the boundary layer parameter predictions obtained for the NACA 4415 aerofoil at 14.5 degrees, for transition just prior to separation, and for the separated flow velocity distribution given by Horton.

The effect which such a calculation has on the boundary layer development towards separation is illustrated in Fig. 11. It may be observed that the result of the reduced boundary layer thickness, associated with the bubble calculation, is to reduce the form parameter growth and, hence, delay the onset of separation. This reduced separation, causes an increase in the predicted lift coefficient which, as may be remembered from the introduction, is opposite to that expected for this aerofoil. This, however, does not invalidate the initial speculation, but, rather, warrants reconsideration of the underlying assumptions embedded in the model.

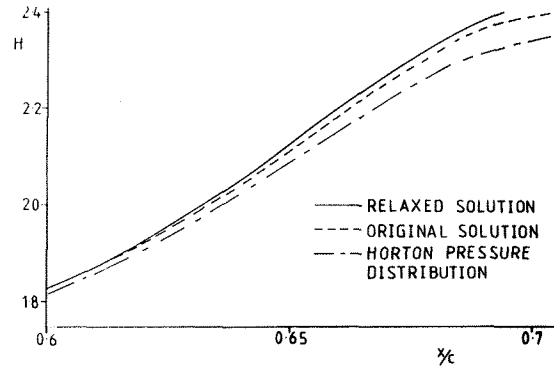


FIGURE 11. Form parameter development towards separation for the NACA 4415 aerofoil with three different transition conditions.

Of particular importance is the sharpness of the form parameter peak, associated with the free shear layer transition, when compared with experiment and inverse schemes. This feature is a consequence of the strict adherence to the pressure distribution of Horton coupled with a fixed transition point. To investigate the effect of this constraint, realistic relaxation of the sharp corner on the pressure distribution was tried (Fig. 12.) with the fixed transition point retained.

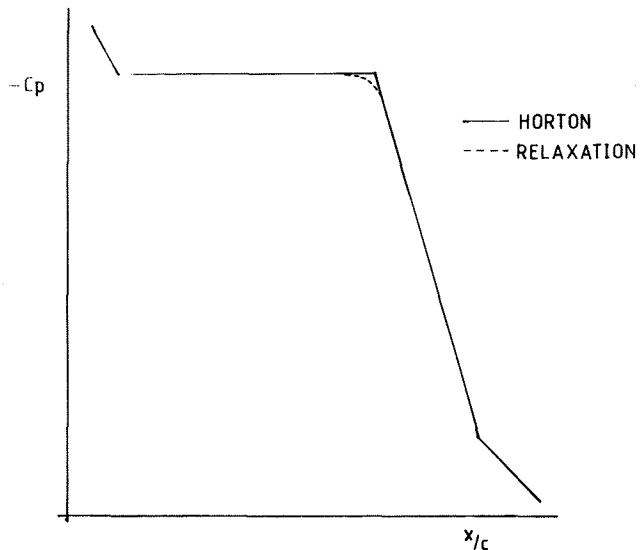


FIGURE 12. Effect of relaxation on the Horton pressure distribution.

The effect of the constraint relaxation may be observed in Fig. 11. where the growth of the form parameter, towards separation, is enhanced and thus the expected earlier separation realised.

This results in an associated reduction in the value of lift coefficient. If a greater degree of relaxation is continually introduced until no shear layer reattachment is indicated, then a lower limit of calculated lift coefficient may be obtained. This is shown in Fig. 13., where it may be observed that, although some reduction in the lift curve is evident, the calculation still lies above the empirical line. It should, however, be noted that only a very minor modification to the bubble pressure distribution produces this change in lift, and that neither the location of transition or the length of the bubble length were altered.

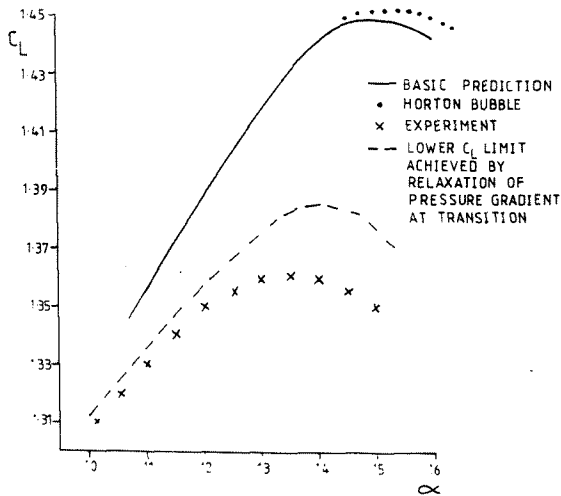


FIGURE 13. Variation of lift near stall associated with the different methods of transition calculation.

It is clear from the above, that the specification of the pressure distribution around the transition region has a significant effect on the direct bubble calculation and the subsequent attached turbulent boundary layer development. It may also be suggested that this finding is equally as significant for inverse calculation schemes where the pressure distribution around transition is strongly dependant on the form of boundary layer transition model adopted. Whether transition is considered to occur at a point or over a specified region, it is clear that the accuracy of the solution obtained via an inverse scheme will be strongly dependent on the validity of the boundary layer empiricism for transitional flows.

It is conceivable that, by further adjustment of the bubble pressure distribution, it may have been possible to obtain good correspondence between experiment and calculation. Indeed, adjustment of the pressure distribution around reattachment, to resemble that produced by some inverse calculations^(?), permits substantially more boundary layer growth after reattachment and

would produce values of lift below those measured by experiment. It is considered, however, that, whilst useful work could be done, such an investigation is beyond the scope of this paper, as a more sophisticated model for the bubble pressure distribution would be required. More work is required, however, before such a routine may be used with any confidence as a design tool.

2.6 Conclusions

1. A direct boundary layer method capable of calculating through separation bubbles has been developed. The technique has been demonstrated to compare well with inverse calculations for a prescribed pressure distribution.
2. The specification of the pressure distribution around the separated shear layer transition region has been demonstrated to be important to the subsequent development of the attached turbulent boundary layer.
3. It is suggested that the accuracy of inverse methods is strongly linked to the boundary layer transition model employed therein.

Acknowledgements

The authors wish to acknowledge the encouragement and support of Professor B.E. Richards of Glasgow University.

References

1. Goldberg, P., 'Upstream History and Apparent Stress in Turbulent Boundary Layers', M.I.T., Gas Turbine Laboratory Rept. No. 85, 1966
2. Nash, J.F., 'Turbulent Boundary Layer Behaviour And The Auxiliary Equation', A.R.C. C.P. 835, 1965
3. Head, M.R., 'Equilibrium and Near-equilibrium Turbulent Boundary Layers', Journal of Fluid Mechanics, Vol. 73, 1976
4. Mueller, T.J., 'Low Reynolds Number Vehicles', AGARDograph No. 288, (February 1985).
5. Coton, F.N., Galbraith R.A.McD., 'A Direct Viscid-Inviscid Interaction Scheme for the Prediction of 2-Dimensional Aerofoil Performance in Incompressible Flow', Glasgow University Aero Rept. No. 8701, 1987
6. Coles, D., 'The Law of the Wake in the Turbulent Boundary Layer', C.I.T. Report, 1955
7. Gleyzes, G., Cousteix, J., Bonnet, J.L., 'A Calculation Method of Leading Edge Separation Bubbles', Numerical and Physical Aspects of Aerodynamic Flow, Vol II, 1984

8. Davis, R.L., et al. 'ALESEP: A Computer Program for the Analysis of Airfoil Leading Edge Separation Bubbles', NASA-CR-172310 1984
9. Kwon, O.K., Pletcher, R.H., 'Prediction of Subsonic Separation Bubbles on Airfoils by Viscous-Inviscid Interaction' Second Symposium on Numerical and Physical Aspects of Aerodynamic Flows', C.S.U., 1983
10. Coton, F.N., 'contributions to the Prediction of Low Reynolds Number Aerofoil Performance', Ph.D. Thesis, University of Glasgow, 1988
11. Leishman, J.G., Galbraith, R.A.McD, Hanna, J., 'Modelling of Trailing edge Separation on Arbitrary Two-Dimensional Aerofoils in Incompressible Flow Using an Inviscid flow Algorithm', Glasgow University Aero report No. 8202 1982
12. Maskew, B., Dvorak, F.A., 'Investigation of Separation Models for the Prediction of C_l max', American Helicopter Society Paper 77-33-01, 1977
13. Le Foll, J., 'A Theory of Representation of the Properties of Boundary layers on a Plane', Proc. Seminar on Advanced Problems in Turbomachinery, V.K.I., 1965
14. Assassa, G.M., Papailiou, K.D., 'An Integral Method for Calculating Turbulent Boundary Layer with Separation', Transactions of the ASME, Vol.100, 1979
15. Kuhn, G.D., Neilsen, J.N., 'Prediction of Turbulent Separated Boundary Layers', AIAA Journal, Vol. 12, no. 7, 1974
16. Head, M.R., 'An Approximate Method for Calculating the Laminar Boundary Layer in Two-Dimensional Incompressible Flow', ARC R & M No. 3123, 1959
17. Roberts, W.B., Calculation of Laminar Separation Bubbles and Their Effect on Airfoil Performance', AIAA Journal, Vol. 18, 1980
18. Horton, H.P., 'A Semi-Empirical Theory for the Growth and Bursting of Laminar Separation Bubbles', ARC. C.P. No. 1073, 1969
19. Gault, D.E., 'An Experimental Investigation of Regions of Separated Laminar Flow', NACA TN 3505, 1955